Mesoscale modeling of the water liquid-vapor interface: A surface tension calculation

A. Ghoufi*
Institut de Physique de Rennes, UMR CNRS 6251, Université Rennes 1, 263 avenue du Général Leclerc, F-35042 Rennes, France

P. Malfreyt†
Clermont Université, Université Blaise Pascal, Laboratoire de Thermodynamique et Interactions Moléculaires, UMR CNRS 6272, LTIM, BP 10448, F-63000 Clermont-Ferrand, France

(Received 26 November 2010; revised manuscript received 3 February 2011; published 3 May 2011)

We report a mesoscale modeling of the liquid-vapor interface of water. A mesoscopic model of water has been established in dissipative particle dynamics (DPD) to reproduce the interfacial properties of water. The surface tension and coexisting densities are compared between atomistic and mesoscopic simulations. Simple scaling relations have been established to link the atomistic and mesoscopic length and time scales. Our study demonstrates the capability of the DPD method to explore the interfacial properties of a planar water liquid-vapor interface and a water nanodroplet. This constitutes an important step toward the calculation of the surface tension of larger and more complex interfacial systems.

DOI: 10.1103/PhysRevE.83.051601 PACS number(s): 68.03.Cd

I. INTRODUCTION

The knowledge of structural and thermodynamic aspect of aqueous interfaces is a key element for various applications such as energy saving, gas storage, and health. The most important of these interfacial properties is the surface tension driving the mass transport across the surface. The molecular simulation is a powerful technique to characterize the interfacial systems from a structural and energy viewpoints. A key issue when performing simulations of water is the choice of the potential model used to describe the interactions between molecules. As a consequence, several water molecular models and methodologies of two-phase simulations have been developed [1–21] to well predict the surface tension of water. However, the two-phase simulations are much less widespread at the mesoscopic scale. As a result, the physical properties of the water-air interface has been rarely investigated at this scale in spite of a quite attractive challenge to reach these length and time scales.

The dissipative particle dynamics (DPD) method, introduced by Hoogerbrugge and Koelmann [22] in 1992, is a promising technique that might bridge the gap between the atomistic and mesoscopic scales. As a consequence of this coarse graining, the conservative interactions are soft, repulsive, and short-ranged. The soft potential allows for a time step that is up to an order of magnitude larger than those typically used in molecular dynamics (MD) simulations. The model is then computationally cheaper. However, modeling specific molecules with DPD is not an easy task due to the lack of quantitative relation between DPD and atomistic parameters. Important contributions [23–26] were nevertheless proposed in this field and DPD was established to be a powerful method for the modeling of various length and time scales. At the beginning of the DPD method, there was a real need to develop a water bulk model due to a large number of potential applications. Groot *et al.* [23–25] have developed a model based upon the experimental compressibility of water at 298 K. Nevertheless, the thermodynamic and dynamic properties of this model were only reproduced for bulk water at $T = 298$ K. In order to model liquid-vapor interfaces, the original version of the DPD method has been modified to introduce attractive forces that are dependent on the local density. The so-called multibody DPD (MDPD) method has been used to model liquid-vapor interfaces [27–30]. The aim of this communication is to provide a set of MDPD parameters based on the surface tension calculation capable of exploring the interfacial properties of water.

II. SIMULATION DETAILS

We follow the strategy developed by Groot and Rabone [24] consisting of modeling $N_m = 3$ water molecules by one DPD bead (Fig. 1). A bead represents then 90 Å^3. The correspondence between the DPD reduced units and the real units is given in Table I.

In the standard DPD method, particles interact with the force $\mathbf{f}_i$ defined as the sum of three contributions $\mathbf{f}_i = \sum_{j\neq i}(\mathbf{f}_{ij}^C + \mathbf{f}_{ij}^R + \mathbf{f}_{ij}^D)$, where the random $\mathbf{f}_{ij}^R$ and dissipative $\mathbf{f}_{ij}^D$ forces are pairwise additive forces. Within the MDPD technique, the conservative force [27–29,32] is not only dependent on the interparticle separation but also on the local particle density. The resulting conservative force is then expressed as $\mathbf{f}_{ij}^C = A\omega_C(r_{ij})\mathbf{e}_{ij} + B[\bar{\rho}_i + \bar{\rho}_j]\omega_d(r_{ij})\mathbf{e}_{ij}$, where the first term represents an attractive interaction ($A < 0$) and the second many-body term a repulsive interaction ($B > 0$). The weight function $\omega_d(r_{ij})$ is chosen as $\omega_d(r_{ij}) = 1 - \frac{r_{ij}}{r_d}$ if $r_{ij} < r_d$ and $\omega_d(r_{ij}) = 0$ if $r_{ij} > r_d$. r_d defines the range of the repulsive many-body interaction with $r_d < r_c$. r_c is the cutoff radius of the attractive part of $\mathbf{f}_{ij}^C$ and $\bar{\rho}_i$ represents the average local density at the position of the particle i defined as $\bar{\rho}_i = \sum_{j\neq i}\omega_\rho(r_{ij})$. The weight function $\omega_\rho(r_{ij})$ is normalized so that $\int_0^\infty 4\pi r^2\omega_\rho(r)dr = 1$. Its operational expression becomes $\omega_\rho(r_{ij}) = \frac{15}{2\pi r_d^3}(1 - \frac{r_{ij}}{r_d})^2$ if $r_{ij} < r_d$ and $\omega_\rho(r_{ij}) = 0$ if $r_{ij} > r_d$. In our MDPD simulations, the particle mass, the temperature, and interaction range were chosen as units of mass, energy,

*Aziz.Ghoufi@univ-rennes1.fr
†Patrice.Malfreyt@univ-bpclermont.fr

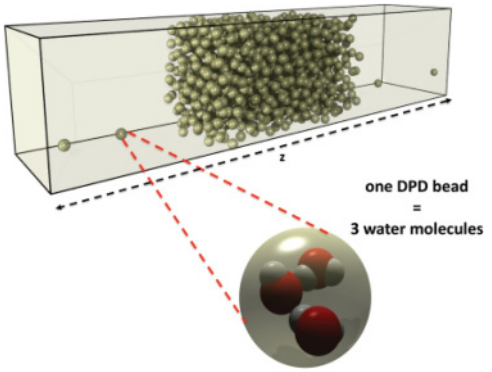

FIG. 1. (Color online) A liquid-vapor interface of DPD particles. The simulation box contains 1000 DPD particles. The z direction is normal to the interface.

and length; hence, $m^* = r_c^* = (k_B T)^* = 1$. The range of the repulsive many-body interaction was put to $r_d = 0.75 r_c$. The equations of motions of the MDPD simulations were integrated using a modified velocity-Verlet algorithm. The time step was $\delta t = 0.01\tau$ and corresponds to a physical value of 6.8 ps (Table I). The equilibration phase was formed by 5×10^5 steps and the average thermodynamic properties were averaged over 10^6 additional steps in the constant-*NVT* ensemble. The corresponding effective simulation time is about 7 μs. The simulation boxes were orthorhombic boxes of dimensions $L_x L_y L_z$. The MDPD simulations used a simulation cell of 1000 DPD beads with $L_x = L_y = 5 r_c$ and $L_z = 22 r_c$. The link with the atomistic scale is carried throughout the molecular simulations of 3000 water molecules. The constant-*NVT* MD simulations were performed with 3000 water molecules in a simulation box with sides of length $L_x = L_y = 35.5$ Å and $L_z = 175$ Å. The water molecules were modeled using the TIP4P/2005 model [4]. The computational procedures (model, methodology) are reported in Ref. [6].

Initially, the A and B parameters of the multibody conservative force were equal to -40 and 25, respectively. The attractive parameter A corresponds to that of the original version of the MDPD method (see Ref. [25] for details). To be in line with the usual DPD simulations we kept fixed the repulsive parameters

TABLE II. Values of surface tension, density, and compressibility calculated from molecular (MC, MD) and mesoscopic (MDPD, MMC) methods with two different definitions. $\gamma_{IK} = \frac{1}{2}\int_{-\infty}^{\infty}[p_N(z) - p_T(z)]dz$ and the working expression of γ_{KB} can be found in Ref. [30]. The experimental surface tension is taken from Ref. [36]. The surface tension and density calculated from MC simulations are taken from Ref. [6], whereas the liquid densities calculated from MD are taken from Ref. [9]. The statistical fluctuations correspond to 4 and 1 mN m^{-1} for the molecular and DPD models, respectively.

Method	γ_{KB} (mN m^{-1})	γ_{IK} (mN m^{-1})	ρ (kg m^{-3})	$\langle\kappa^{-1*}\rangle$
MD	70	69	993	
MC	71	72	99	
MDPD	71	71	994	49
MMC	71	71	994	49
Experiments	72		996	45

at $B = 25$. To decrease the deviation with experiments, we adopt then an optimization procedure consisting in mapping the A parameter on the simulated surface tension at the atomistic scale at only one temperature. We took the route of using the interfacial tension as a fitting property which is a key interfacial property. Other solutions were possible as for instance taking the density and the compressibility as fitting properties. For each set of parameters, a two-phase MDPD simulation is carried out to calculate the surface tension. The iterative optimization [33] gives $A = -50$. The calculated surface tension is then 70.6 mN m^{-1}. We also checked that the predicted density and reduced liquid compressibility (properties not used in the adjustment database) agree very well with experiments, atomistic simulated values (Table II), and values obtained from the equation of state (see Ref. [25] for the α and c fitting parameters) given by $\kappa^{-1*} = \frac{N_m}{\rho^* k_B T \kappa_T} = \frac{1}{k_B T}\left(\frac{\partial p^*}{\partial \rho^*}\right)_{N,T} = 1 + \frac{2\alpha A \rho^*}{k_B T} + \frac{2\alpha B r_d^4 (3\rho^{*2} - 2c\rho^*)}{k_B T}$.

III. RESULTS AND DISCUSSIONS

The surface tensions calculated from the Kirkwood-Buff [34] and Irving and Kirkwood [35] definitions are given in

TABLE I. Correspondence between the DPD parameters in reduced units represented with a star notation and the real values. r_c, ρ, p, and γ correspond to the cutoff radius, density, pressure, and surface tension, respectively. κ^{-1*} is the dimensionless isothermal compressibility in reduced DPD units and κ_T is the usual isothermal compressibility. V is the volume of one water molecule (30 Å^3), M the molar weight of a water molecule (18 g mol^{-1}), N_A is Avogadro's number, k_B is Boltzmann's constant, T is 298 K. n is the number of water molecules in a volume of 1 m^3. The experimental value [31] of κ_T is equal to 4.5×10^{-10} Pa^{-1} at 298 K. The reduced time step δt^* is calculated from the ratio of the diffusion coefficient D_{bead} of a DPD bead to that of water $D_{water} = 2.43 \times 10^{-5}$ cm^2 s^{-1}.

DPD			Physical units	
Parameter	Value	DPD → Real units	Parameter	Value
Bead	1	N_m	3	3 H_2O
r_c^*	1	$(\rho^* N_m V)^{1/3}$	r_c	8.52 Å
ρ^*	6.88	$\rho^* N_m M / N_a r_c^3$	ρ	997 kg m^3
p^*	0.1	$p^* k_B T / r_c^3$	p	6.7 MPa
γ^*	12.4	$\gamma^* k_B T / r_c^2$	γ	70.6 mN m^{-1}
κ^{-1*}	48.0	$N_m/(n k_B T \kappa^{-1*})$	κ_T	4.5×10^{-10} Pa^{-1}
δt^*	0.01	$N_m D_{bead} r_c^2 / D_{water}$	Δt	6.8 ps

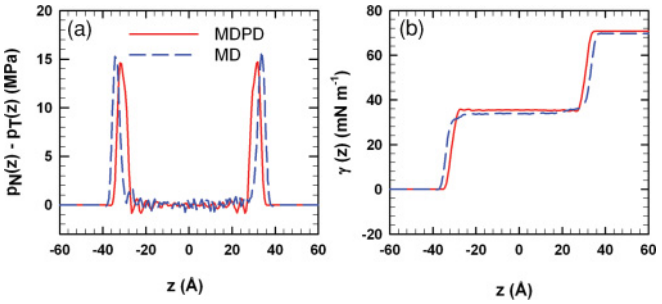

FIG. 2. (Color online) (a) Difference between the profiles of the normal and tangential components of the pressure tensor calculated from MDPD and MD simulations for water at 298 K. (b) Integral of $p_N(z)$ and $p_T(z)$ as a function of z at 298 K.

Table II for the MDPD and MD simulations. We add for completeness the surface tensions calculated from Monte Carlo molecular simulations and Monte Carlo multibody simulations (MMC) (see Ref. [30] for a description of the MMC method). The surface tensions match very well between the different methods and compare very well with experiments.

In Fig. 2(a), we plot the difference between the normal and tangential pressure profiles which is known to be a key element to checking the validity of the calculation concerning the stabilization of the interfaces, the independence between the two interfaces, and the constancy $[p_N(z) - p_T(z) \simeq 0]$ of the profile in the bulk phases. This profile is shown in Fig. 2(a) for the MDPD and MD methods. The profile calculated from MDPD is scaled by the relations given in Table I for the pressure and the z dimension. We observe that the profiles match very well with two independent interfaces and well-developed bulk phases. The integral of this profile is then given in Fig. 2(b) and establishes that the profiles of the surface tension are identical within the statistical fluctuations for the molecular and the mesoscopic methods.

The molecular density profiles of the two-phase simulations are also compared in Fig. 3. The density profiles calculated from MDPD and MMC methods are changed by applying the simple scaling relation for ρ (Table I). Figure 3(a) shows that the profiles indicate the same water density in the liquid phase. The profiles calculated from the mesoscopic methods

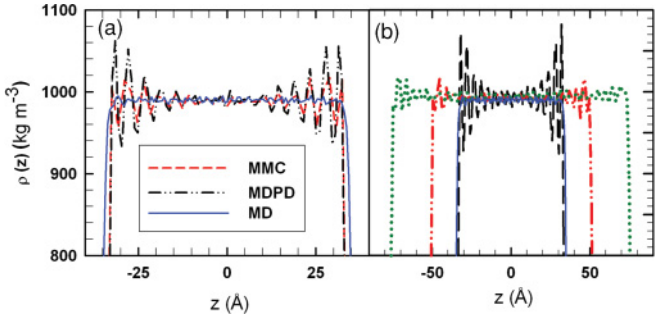

FIG. 3. (Color online) (a) Density profiles of water as a function of z calculated from the MD, MDPD, and MMC mesoscale methods. (b) Different density profiles as a function of the number of DPD beads: 1000 (dashed line), 3000 (dashed-dotted line), 10 000 (dotted line). The profile calculated from MD simulations is given for comparison (solid line).

TABLE III. Surface tension values (mN m^{-1}) calculated using various water models at three temperatures. Experimental surface tensions of water were taken from Ref. [36]. The surface tensions of the TIP3P, SPC, SPC/E, TIP4P, TIP5P, and TIP6P models were taken in Ref. [8], while that calculated using TIP4P/2005 is taken from Ref. [9]. The surface tension of water using the TIP4P/2005 potential at 275 K is calculated from Eq. (6) of Ref. [9]. The temperatures 275 K and 325 K correspond to reduced DPD temperatures of 0.92 and 1.09, respectively. For these two temperatures, the DPD simulations are purely predictive. For the MMC simulations we give the surface tension of three system sizes: 1000, 3000, and 10 000 DPD beads. The statistical error bars are 4 and 1 mN m^{-1} for the molecular and DPD models, respectively.

Model	275 K	298 K	325 K
	Atomistic model		
TIP3P	54	49	44
SPC	60	53	49
SPC/E	64	61	58
TIP4P	61	55	51
TIP5P	57	52	46
TIP6P	65	62	55
TIP4P/2005	73	69	65
	Mesoscopic model		
MMC-1000	73	71	68
MMC-3000		71	
MMC-10000		73	
Experiments	75	72	68

exhibit higher oscillations due to the combination of strong attractive and repulsive interactions. These oscillations have already been studied by Warren [29] with a less attractive set of parameters ($a_{ij} = -40$, $b_{ij} = 40$). Figure 3(b) shows the water density profiles calculated from MDPD simulations with different system sizes. By increasing the number of DPD particles (from 1000 to 10 000 beads), the oscillatory effect is decreasing. This means that the magnitude of the oscillatory effect is related to size effects in the system. The capillary effect is found to vanish for larger box sizes (Fig. 3(b)) despite a residual wave of capillarity. From Table III we check that the value of the surface tension is not significantly affected by the change in the number of particles. In fact, the change in the surface tension with the system-size is of the order of magnitude of the estimated error in the simulation. As mentioned previously in Refs. [29,30] the MDPD potential can only be used in interfacial systems with a poor vapor phase because of the strong attractive contribution of the potential. It means that the calculation of the surface tension at high temperatures is not possible from MDPD simulations. However, as shown in Table III from 275 K to 325 K, the MDPD model developed here gives a deviation of 3.5% with respect to experiments, whereas atomistic models can lead to deviations greater than 20%. We show the ability of the MDPD water to reproduce the surface tension of water at temperatures close to 298 K.

As a new example of application, we extend this study to the calculation of the surface tension of a water nanodroplet at four different sizes R of the drop. First, the planar limit was obtained with 30 000 real water molecules. Figures 4(a)

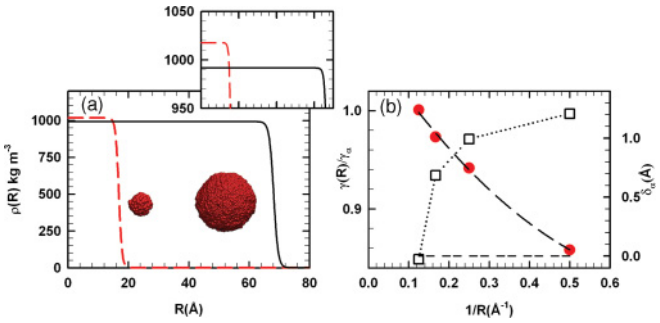

FIG. 4. (Color online) (a) Radial density profiles of water for two different radii. These profiles were obtained using a hyperbolic fitting. The inset is an enlargement in the range of 1000 kg m^{-3}. (b) Ratio of the surface tension of the nanodroplet to the surface tension (γ_∞) of the planar limit as a function of $1/R$. The solid line corresponds to the fit to the simulated surface tension by the $1 - 2\delta_\infty/R + 2(l_s/R)^2$ expression (solid circles on the left axis). The Tolman length, δ_∞, is shown as a function of $1/R$ on the right axis (open squares). The $\delta_\infty = 0$ limit is shown as a double-dashed line (right axis).

and 4(b) show the impact of the drop size on the density and surface tension properties. These dependences were already observed on simple molecular fluid [37–39] and confirm that the physics of such systems is well reproduced by the water DPD model.

The Tolman length, δ_∞ is defined by $\gamma(R)/\gamma_\infty = 1 - 2\delta_\infty/R + 2(l_s/R)^2$, where γ_∞ is the surface tension for the planar liquid-vapor interface and l_s is related to the rigidities k and $\bar{k}$ by $l_s^2 = 2\delta_\infty^2 - \frac{2k+\bar{k}}{2\gamma_\infty}$, where k is the bending rigidity constant and $\bar{k}$ the rigidity constants associated with Gaussian curvature. Figure 4(b) shows the dependence of the surface tension on the drop radius R and the resulting fit to the simulated data by the $\gamma(R)/\gamma_\infty = 1 - 2\delta_\infty/R + 2(l_s/R)^2$ expression. The regression gives $l_s \approx 0$. The linear approximation $\gamma(R)/\gamma_\infty = 1 - 2\delta_\infty/R$ commonly used for sufficiently large drops is reproduced by our DPD simulations. A negative Tolman length $\delta_\infty \approx -0.1$ Å is found for the largest drop size ($R = 68$ Å), indicating that the surface tension $\gamma(R)$ is slightly larger than γ_∞. From the mean-field predictions for the penetrable sphere model [39,40], δ_∞ is expected to be negative for the largest drop sizes while the vast majority of molecular computer simulations studies [38] predict a positive Tolman length. This is in line with recent studies on the nanoscale drops [38].

IV. CONCLUSIONS

An important conclusion of this work is that the DPD method is capable of reproducing the interfacial thermodynamic properties and the physics of interfacial water systems. The computational cost of a DPD simulation is 20 times smaller than that of the molecular methods for the same real simulation time. Simple scaling relations between DPD parameters and physical units have been established here for water. This constitutes an important step toward the prediction of interfacial properties of molecular systems from mesoscopic simulations. It can open the way of investigating binary mixtures, micelles, and nanoparticles at the liquid-air interfaces for which the molecular simulations [41,42] are really time consuming.

ACKNOWLEDGMENTS

This work was supported in part by the French Agence Nationale de la Recherche (ANR), under Grant No. SUSHI (ANR-07-BLAN-0268) "SimUlation de Systèmes Hétérogènes et d'Interfaces." This work was also granted access to the HPC resources of IDRIS under the allocation 2010-i2010092119 made by GENCI (Grand Equipement National de Calcul Intensif).

[1] W. L. Jorgensen, J. Chandrasekhar, J. D. Madura, R. W. Impey, and M. L. Klein, J. Chem. Phys. **79**, 926 (1983).
[2] H. J. C. Berendsen, J. R. Grigera, and T. P. Straatsma, J. Phys. Chem. **91**, 6269 (1987).
[3] M. W. Mahoney and W. L. Jorgensen, J. Chem. Phys. **112**, 8910 (2000).
[4] J. L. F. Abascal and C. Vega, J. Chem. Phys. **123**, 234505 (2005).
[5] J. Alejandre, D. J. Tildesley, and G. A. Chapela, J. Chem. Phys. **102**, 4574 (1995).
[6] A. Ghoufi, F. Goujon, V. Lachet, and P. Malfreyt, J. Chem. Phys. **128**, 154716 (2008).
[7] P. J. Veld, A. E. Ismail, and G. S. Grest, J. Chem. Phys. **127**, 144711 (2007).
[8] F. Chen and P. E. Smith, J. Chem. Phys. **126**, 221101 (2007).
[9] C. Vega and E. de Miguel, J. Chem. Phys. **126**, 154707 (2007).
[10] B. Shi, S. Sinha, and V. Dhir, J. Chem. Phys. **124**, 204715 (2006).
[11] J. Alejandre and G. A. Chapela, J. Chem. Phys. **132**, 014701 (2010).
[12] M. Gonzalez-Melchor, P. Orea, J. Lopez-Lemus, F. Bresme, and J. Alejandre, J. Chem. Phys. **122**, 094503 (2005).
[13] P. Orea, J. Lopez-Lemus, and J. Alejandre, J. Chem. Phys. **123**, 114702 (2005).
[14] J. R. Errington and D. A. Kofke, J. Chem. Phys. **127**, 174709 (2007).
[15] F. Biscay, A. Ghoufi, F. Goujon, V. Lachet, and P. Malfreyt, J. Chem. Phys. **130**, 184710 (2009).
[16] A. Trokhymchuk and J. Alejandre, J. Chem. Phys. **111**, 8510 (1999).
[17] F. Goujon, P. Malfreyt, J. M. Simon, A. Boutin, B. Rousseau, and A. H. Fuchs, J. Chem. Phys. **121**, 12559 (2004).
[18] G. J. Gloor, G. Jackson, F. J. Blas, and E. de Miguel, J. Chem. Phys. **123**, 134703 (2005).
[19] C. Ibergay, A. Ghoufi, F. Goujon, P. Ungerer, A. Boutin, B. Rousseau, and P. Malfreyt, Phys. Rev. E **75**, 051602 (2007).
[20] F. Goujon, P. Malfreyt, A. Boutin, and A. H. Fuchs, Mol. Simul. **27**, 99 (2001).
[21] F. Goujon, P. Malfreyt, A. Boutin, and A. H. Fuchs, J. Chem. Phys. **116**, 8106 (2002).

[22] P. J. Hoogerbrugge and J. M. V. A. Koelman, Europhys. Lett. **19**, 155 (1992).
[23] R. D. Groot and P. B. Warren, J. Chem. Phys. **107**, 4423 (1997).
[24] R. D. Groot and K. L. Rabone, Biophys. J. **81**, 725 (2001).
[25] R. D. Groot, J. Chem. Phys. **118**, 11265 (2003).
[26] L. Rekvig, B. Hafskjold, and B. Smit, Langmuir **20**, 11583 (2004).
[27] I. Pagonabarraga and D. Frenkel, J. Chem. Phys. **115**, 5015 (2001).
[28] S. Y. Trofimov, E. L. F. Nies, and M. A. Michels, J. Chem. Phys. **117**, 9383 (2002).
[29] P. B. Warren, Phys. Rev. E **68**, 066702 (2003).
[30] A. Ghoufi and P. Malfreyt, Phys. Rev. E **82**, 016706 (2010).
[31] F. J. Millero, R. W. Curry, and W. Drost-Hansen, J. Chem. Eng. Data **14**, 422 (1969).
[32] S. Y. Trofimov, E. L. F. Nies, and M. A. J. Michels, J. Chem. Phys. **123**, 144102 (2005).
[33] A. Ghoufi, D. Morineau, R. Lefort, and P. Malfreyt, J. Chem. Theory Comput. **6**, 3212 (2010).
[34] J. G. Kirkwood and F. P. Buff, J. Chem. Phys. **17**, 338 (1949).
[35] J. H. Irving and J. G. Kirkwood, J. Chem. Phys. **18**, 817 (1950).
[36] Data taken from the staturation properties of water at theNIST Standard Reference Database [http://webbook.nist.gov].
[37] P. Schofield and J. R. Henderson, Proc. R. Soc. London A **379**, 231 (1982).
[38] J. Sampayo, A. Malijevský, E. A. Muller, E. de Miguel, and G. Jackson, J. Chem. Phys. **132**, 141101 (2010).
[39] B. Block, S. Das, M. Oettel, P. Virnau, and K. Binder, J. Chem. Phys. **133**, 154702 (2010).
[40] S. J. Hemingway, J. R. Henderson, and J. S. Rowlinson, Symp. Chem. Soc. Faraday **16**, 33 (1981).
[41] F. Biscay, A. Ghoufi, V. Lachet, and P. Malfreyt, J. Chem. Phys. **131**, 124707 (2009).
[42] F. Biscay, A. Ghoufi, V. Lachet, and P. Malfreyt, J. Phys. Chem. B **113**, 14277 (2009).